PHOTONICS Research

Evanescent-wave pumped single-mode microcavity laser from fiber of 125 μm diameter

YUCHEN WANG,[1,2] SHU HU,[1] XIAO YANG,[3] RUIZHI WANG,[1] HENG LI,[1] AND CHUANXIANG SHENG[1,*]

[1]School of Electronic and Optical Engineering, Nanjing University of Science and Technology, Nanjing 210094, China
[2]School of Science, Qingdao University of Technology, Qingdao 266520, China
[3]Faculty of Electronic Information Engineering, Huaiyin Institute of Technology, Huaian 223003, China
*Corresponding author: cxsheng@njust.edu.cn

Received 26 December 2017; revised 28 January 2018; accepted 30 January 2018; posted 1 February 2018 (Doc. ID 318398); published 27 March 2018

A microcavity laser based on evanescent-wave-coupled gain is formed using a silica fiber with a diameter of 125 μm in a rhodamine 6G ethanol solution. When the fiber is sticking to the cuvette wall by capillary force, using the excitation of a 532 nm nanosecond pulsed laser, single-mode laser emission is observed. While increasing the distance between the fiber and the cuvette wall, the typical multi-peak whispering-gallery-mode (WGM) laser emission can also be demonstrated. On the other hand, while increasing the refractive index of the solution by mixing ethanol and ethylene glycol with different ratios as a solvent, the single-mode emission would evolve to multi-peak WGM laser emission controllably.

OCIS codes: (140.3945) Microcavities; (140.3570) Lasers, single-mode; (230.3120) Integrated optics devices.

https://doi.org/10.1364/PRJ.6.000332

1. INTRODUCTION

Whispering-gallery mode (WGM) optical microcavities have found potential applications in sensing [1–4], integrated optics [5,6], lasing [7–9], and other research areas [10] due to their small volumes and ultrahigh Q (quality factor) values. WGMs are formed in symmetric cavities such as microspheres [11,12], microdisks [13,14] and microrings [15,16] by total reflection on the interface between the high refractive index (RI) and low RI materials. However, WGMs were usually multimode, which limited their application. Many research groups had made efforts to achieve single-mode emission in WGMs. For example, it had been reported that a single-mode WGM laser can be realized by coupled cavities taking advantage of the Vernier effect [17–20] and parity-time symmetry breaking [21,22]. These methods usually needed complicated and rigorous fabrication along with precise operation. Another noticeable method was to reduce the size of the micro-cavity to expand the free spectral range, so that only a single laser line was left [11], but this method will increase the lasing threshold due to small round trip gain. Other methods included modifying the spatial gain profiles of micro-resonators by engineering the pump intensity, which also needed a complicated optical setup to obtain laser-interference excitation [23]. At the same time, optofluidic lasers, which combined a liquid gain medium and an optical cavity for optical feedback to achieve laser emission, have attracted much attention recently [24–33]. In particular, the WGMs could be formed in an optofluidic resonator due to the evanescent wave in gain solution outside of the cavity. However, to the best of our knowledge, only multimode WGM emissions had been reported in optofluidic lasers [24,29,34–36].

In this work, a microcylinder cavity was formed by using a fiber with a diameter of 125 μm, which was rested on the wall of a quartz cuvette containing 5 mg/mL rhodamine 6G (Rh6G) ethanol solutions. Being excited by a 532 nm nanosecond pulsed laser, we observed both single-line emission and multimode WGM emission, which resulted from the evanescent-wave coupling between the gain molecules and the resonator modes. More importantly, the emission modes can be simply controlled by adjusting the distance between the fiber and the wall of cuvette, as well as the refractive index of the solution.

2. EXPERIMENTAL SECTION

A. Sample Preparation

The gain solution was prepared by dissolving 5 mg Rh6G in 1 mL ethanol and was put in a quartz cuvette. The refractive index of the solvent is 1.361; the RIs of the cuvette and fiber are both ~1.455. A segment of fused-silica optical fiber with diameter of 125 μm was used as a cylindrical cavity. The protecting layer of the optical fiber was removed carefully to avoid the damage to the fiber surface; then the bare fiber was cleaned carefully by ethanol. After the fiber was dried, it was

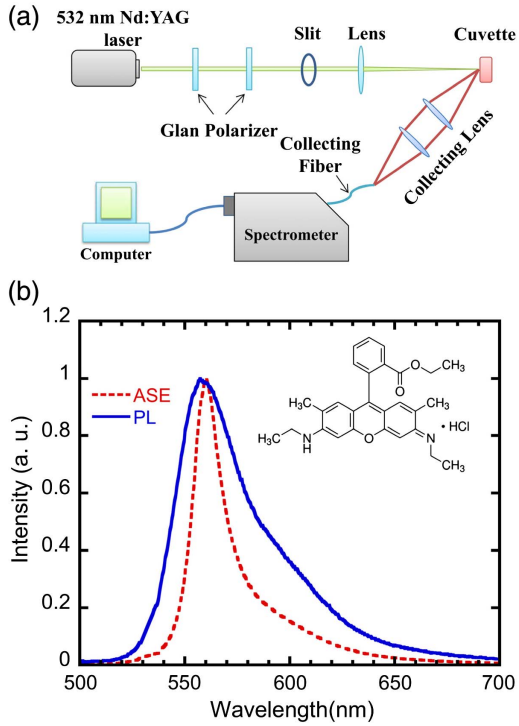

Fig. 1. (a) Diagram of the experimental setup; (b) comparison between photoluminescence (PL) spectrum excited by a continuous wave laser at 20 mW/cm^2 and the amplified spontaneous emission (ASE) excited by a 10 ns pulsed laser at 96.5 μJ/pulse of 5 mg/mL ethanol solution of rhodamine 6G (Rh6G). Inset is the molecular structure of Rh6G.

dipped into the solution vertically. Due to the capillary force, the fiber was rested against the cuvette front wall with a very thin layer of solution between them.

B. Optical Setup

The experimental setup is shown in Fig. 1(a). An Nd:YAG 532 nm pulsed laser was used as the excitation source (~10 ns pulse duration, 10 Hz repetition rate). The laser beam was focused by a lens with focus length of 10 cm for obtaining a circle spot with diameter of ~100 μm. A circle slit was added before the lens to obtain a uniform speckle. Two polarizers in series were used as an attenuator for adjusting the laser intensity and also for keeping the polarization of the excitation laser parallel to the fiber, which is labeled as a transverse-magnetic (TM) wave compared to the direction of the fiber axis. The polarization of emission was also checked. If the polarization of emission was perpendicular (parallel) to the axis of fiber, we labeled it as TE (TM) accordingly, where TE means transverse-electric. A couple of lenses were used to collect the output light of the WGM using back-scattering geometry. A spectrometer mounted with a charge-coupled device (CCD) was used to disperse the output light and to record the spectrum. The resolution of the system is 0.1 nm, which was measured by a He–Ne laser.

3. RESULTS AND DISCUSSION

We measured the photoluminescence (PL) spectrum of the 5 mg/mL rhodamine 6G ethanol solution using a 532 nm continuous wave (CW) laser with an intensity of 20 mW/cm^2. The emission was collected with back-scattering geometry to avoid self-absorption. As shown in Fig. 1(b), the PL spectrum contains a main peak at 558.4 nm and a shoulder at ~600 nm. The broad spectrum has full width at half-maximum (FWHM) of 41.6 nm. When the solution was excited by a focused 532 nm pulsed laser with beam diameter of ~0.1 mm, as the pump intensity increased, spectral narrowing could be observed at ~560 nm, and the FWHM of the spectrum was decreased to 17.5 nm at pump energy of 96.5 μJ/pulse [Fig. 1(b)]. However, we did not observe any random lasing at any excitation energy (up to 200 μJ/pulse) in this configuration.

When the same excitation beam was moved to the fiber in the solution, because the refractive index of the ethanol (n_1≈1.361) is smaller than that of the fiber (n_2≈1.455), WGM laser emission based on evanescent-wave-coupled gain was expected to be achieved, as described in Ref. [27]. However, it was surprising that single-line laser-like emission was generally observed in our measurements, as shown in Fig. 2(a). The configuration of the fiber in solution was illustrated in Fig. 2(a) left inset, in which the silica fiber is sticking on the surface of the cuvette wall by capillary force [34]. When the pump energy exceeds the threshold energy of 1.2 μJ/pulse, a laser-like emission emerges at 588.40 nm, instead of a WGM laser emission characterized with a multimode lasing spectrum from the cavity

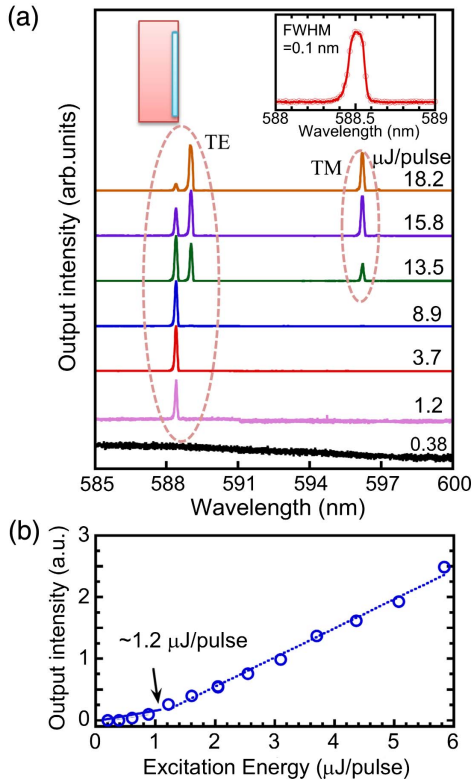

Fig. 2. (a) Emission spectra of a 5 mg/mL Rh6G ethanol solution with a fiber at various excitation intensities. Left inset: sample configuration; the bare fiber rests on the cuvette wall vertically by capillary force. Right inset: emission spectrum excited at 3.7 μJ/pulse. TE, transverse electric; TM, transverse magnetic. (b) Integrated intensity of the emission as a function of excitation pulse energy, indicating a threshold behavior.

of 125 μm diameter fiber [27,34–36]. The FWHM of laser line is about 0.1 nm (right inset), which is the same as the system resolution. When the intensity is increased to 13.5 μJ/pulse, a second peak at 589.02 nm appears, and the free spectrum range ($\Delta\lambda$) is about 0.62 nm. The integrated emission intensity varying with pump energy is shown in Fig. 2(b), which shows the threshold is about 1.2 μJ/pulse. In WGM the laser line spacing $\Delta\lambda$ is given by $\lambda^2/\pi nD = 0.61$ nm, where n is 1.455 for the fiber; this is very close to the $\Delta\lambda$ obtained from the experimental results shown in Fig. 2(a). Therefore, we suggest that the single-mode emission should result from one mode of the WGMs in a microcavity.

Moreover, a third lasing peak emerges at 596.2 nm with the same polarization of the excitation beam when the excitation intensity is above 13 μJ/pulse, which supplies additional evidence that the single-line emission is not artifact from the scattering of the excitation laser. Nevertheless, in Fig. 2(a), no typical multimode WGM laser with a set of evenly spaced narrow lines was observed [34–38]. In addition, single-line emission could be observed at different positions of the fiber and in different samples under similar excitation intensities (Fig. 3), in which the emission wavelengths could be the same or be slightly different. We also found that there is no laser-like emission without fiber in solution, no matter how much pulse energy of the excitation laser, excluding the possibility of random lasing due to the waveguide effect between solution and cuvette [39].

It is noteworthy that not all fibers support the single-line emission. Actually, well-discussed multimode WGM emission [34] was observed in a portion of fiber samples (3 out of 9). Normally, we found the fibers supporting multimode WGM emission were not cleaned thoroughly or were damaged in the process of removing the coating layer, suggesting that the fiber may not stick to the cuvette wall well enough.

To investigate the origin of the single-mode emission, we prepared samples by removing the coating layer of the fiber just at one end. The configuration of the fiber in solution is shown in Fig. 4(a). Compared to the sample configuration shown in Fig. 2(a) left inset, the bare fiber in solution only sticks to the cuvette wall well at the bottom end, illustrated as position 2 in

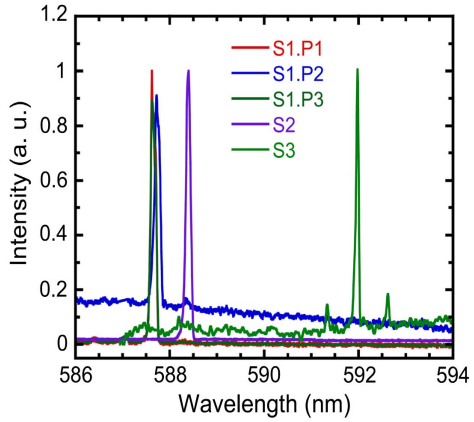

Fig. 3. Single-mode emission from various samples and from various excitation positions in the same sample, all excited using similar pulse energy (~10 μJ/pulse). S1 (2, 3): sample 1 (2, 3). S1. P1(2, 3): position 1 (2, 3) in sample 1.

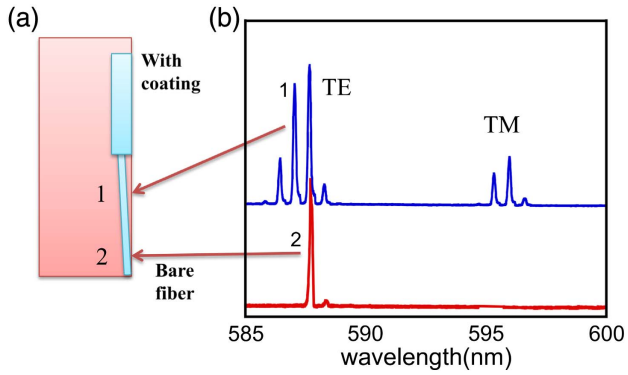

Fig. 4. (a) Scheme of a fiber with coating layer at one end in the 5 mg/mL Rh6G ethanol solution. Two positions on the fiber are marked as 1, 2, respectively; (b) corresponding spectrum excited at two positions by a nanosecond (ns) pulsed laser at pump energy of ~8 μJ/pulse.

Fig. 4(a). When the fiber is excited at position 2, single-line emission is obtained at proper excitation intensities. As the excitation point moves up to the top end of the glass fiber, as illustrated at position 1 in Fig. 4(a) where the bare fiber and the cuvette wall should be separated due to the segment of coating, two groups of multimode WGM emission were observed. The group of emission lines centered at ~587 nm is in TE mode, and the other centered at ~596 nm is in TM mode. Note that the polarization of excitation is also TM. The phenomena are repeatable, suggesting that generation of the single-mode laser may be related to the leakage from the fiber to the cuvette wall when the fiber is sticking well to the cuvette; in other words, the distance between them is small. Moreover, the similarity between the polarization of single-mode and multimode emission supplies additional evidence that the single-mode emission results from one of the WGMs.

To prove our assumption, and more importantly, to achieve WGM emission with controllability, after removing the coating layer of the fiber, we dipped and coated the two ends of a bare silica fiber into 5 mg/mL polymethyl methacrylate (PMMA) toluene solution. After the fiber was dried, PMMA film with a thickness of roughly 1 μm was coated at both ends. When this fiber was put in the solution, in the middle of the fiber without PMMA layer, the bare fiber was separated from the cuvette wall, as illustrated in Fig. 5(a) left inset. With the thickness of coating PMMA larger than the wavelength, the leaking from the WGM mode to cuvette should be ignorable. Therefore, we got a true cylindrical microcavity laser based on evanescent-wave-coupled gain when the fiber was excited by a pulsed laser. As the excitation energy was increased to be more than the threshold energy of 3.8 μJ/pulse, a typical multimode [38] with evenly spaced WGM laser lines was observed ($\Delta\lambda \sim 0.62$ nm); meanwhile, the output integrated intensity increased sharply with the excitation intensity shown in Fig. 5(b). We did not observe single-line emission at any pulse energy in this configuration. This result indicates that single-mode emission may be attributed to the loss modulation due to the optical leakage from the fiber to the cuvette front wall, which selectively amplifies one or a few of WGMs.

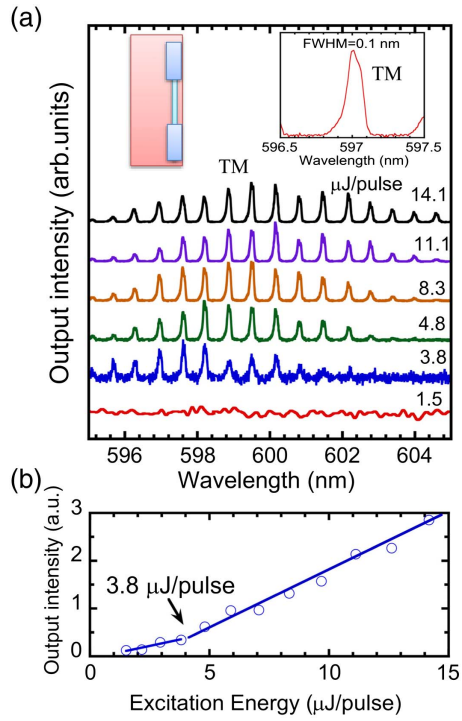

Fig. 5. (a) WGM spectra at various excitation intensities from a fiber in a 5 mg/mL Rh6G ethanol solution. Sample configuration was schematically shown in the left inset, with a bare fiber being coated with PMMA (~thickness of 1 μm) at both ends. Right inset: typical emission spectrum of one WGM mode with FWHM of 0.1 nm; (b) integrated intensity of the emission as a function of excitation pulse energy, indicating a threshold behavior.

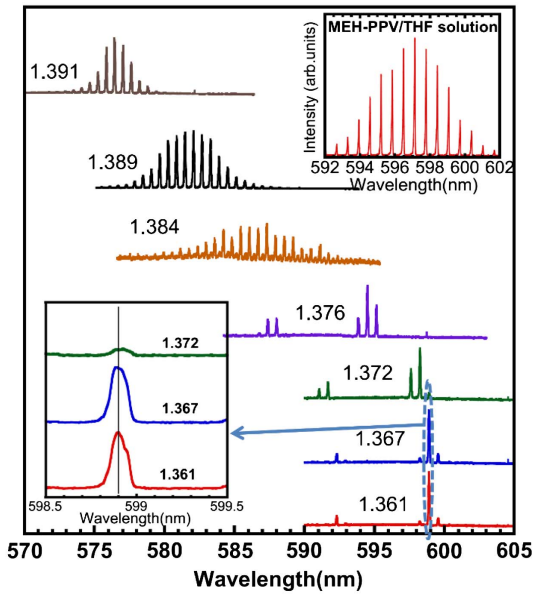

Fig. 6. WGM spectra of a fiber in 5 mg/mL Rh6G solution of mixed ethanol and ethylene glycol with different ratios. The pump energy is ~10 μJ/pulse; in this configuration, the fiber sticks to the cuvette wall. The corresponding refractive indexes are marked at each spectrum. The single-mode emission spectra, which are circled, are also zoomed to show the lack of spectral shift (left inset). Right inset is the WGM emission from a bare fiber in MEH-PPV/THF solution using the same configuration.

We noticed that the peak position of each WGM does not shift with the pump intensity. On the contrary, in the normal WGM laser with a microcavity made of gain medium, the peak position will shift with pump intensities because the refractive index of the gain medium can be modified at high excitation intensities [37,38]. Actually, the single-mode emission shown in Fig. 2(a) also presents fixed emission wavelengths at various pump intensities. This is because the gain materials were excited by the evanescent field region outside the laser cavity completely. The high stability of emission wavelengths is a big advantage for the evanescent-wave-coupled gain approach to achieving a WGM laser, being very crucial for the application in integrated optics [40].

In this work, now we could conclude the extension of an evanescent wave between the fiber and the cuvette wall plays an important role in determining the lasing modes. Besides the distance, another important parameter influencing the leakage of an evanescent wave is the difference of the RIs between solution and fiber [41]. To investigate the effect of RI differences on single-mode emission, 60 μL 5 mg/mL Rh6G ethylene glycol solution ($n_1 = 1.43$) was added into 600 μL 5 mg/mL Rh6G ethanol solution ($n_2 = 1.361$) every time, so we can get solutions of which the refractive index increases gradually, but keeps the same concentration of the gain material. As shown in Fig. 6, the refractive index was calculated by $n_{\text{mix}}^{2/3} = c_1 n_1^{2/3} + (1 - c_1) n_2^{2/3}$, where n_1 and n_2 are the refractive indexes of ethylene glycol and ethanol, respectively; c_1 is the volume ratio of ethylene glycol in a mixed solution; and n_{mix} is the refractive index of the mixed solution, which is marked at the corresponding spectrum shown in Fig. 6. First, we obtained single-line emission in Rh6G ethanol solution, in which the fiber was sticking to the cuvette wall. This is the same configuration as in Fig. 2(a). Then the ethylene glycol dye solution was added into the solution slowly each time. After several minutes' waiting for it to mix well, the emission spectra were measured under the same excitation intensity. As the refractive index was increased to be more than 1.385, the multimode emission was achieved. Summarily, in Fig. 6, we show that single-line emission evolves dramatically to a multimode WGM laser as the RI of the solution is increased.

To check the influence of the refractive index of the solution, we further measured another well-known gain material, namely, poly[2-methoxy-5-(2-ethylhexyloxy)-1,4-phenylenevinylene] (MEH-PPV), which, however, cannot be dissolved by ethanol. We tried toluene (RI = 1.496), chlorobenzene (RI = 1.523), and tetrahydrofuran (THF) (RI = 1.405) as the solvent; only the RI of the THF is smaller than that of the fiber. Therefore, it is not surprising that we observed WGM emission only in the MEH-PPV/THF solution with fiber, as shown in Fig. 6 right inset. However, because the RI of THF is larger than 1.4, we did not observe any single-mode emission in the MEH-PPV/THF solution in any sample, which is consistent with the measurements of Rh6G solution shown in Fig. 6.

It is obvious that multi-peak WGM emission blueshifts while RI is increasing, which is consistent with previous

experimental results [27]. According to the laser model introduced also by Ref. [27], an evanescent-wave pumped microcavity laser will be lasing at λ for which the function of $\gamma(\lambda)$ is minimum. $\gamma(\lambda)$ is the fraction of the excited molecules at the laser threshold, which can be written as [27]

$$\gamma(\lambda) = \frac{\frac{2\pi m}{\lambda \eta Q n_t} + \sigma(\lambda)}{\sigma(\lambda) + \sigma_e(\lambda)}, \quad (1)$$

where n_t is the total number density of the molecules; η is the occupation factor, which is defined as the fraction of the evanescent field volume to that of the whole WGM; Q is the quality factor of the cavity; and $\sigma(\lambda)$ and $\sigma_e(\lambda)$ are the stimulated absorption and emission cross section of the dye molecules, respectively. m is the ratio between the refractive indices of fiber and solution. $\sigma(\lambda)$ and $\sigma_e(\lambda)$ are assumed to be no change for different refractive indices in solution. Therefore, the function $\gamma(\lambda)$ depends mainly on the value of $Q_{\text{solution}} = \eta Q$, which decreases as the RI of the solution increases (Δn between the solution and fiber decreases) [27]. Figure 7 shows the calculated $\gamma(\lambda)$ for various values of $Q_{\text{solution}} = \eta Q$. The $\sigma(\lambda)$ was measured by a spectrometer; the $\sigma_e(\lambda)$ was approximated by the CW PL of Fig. 1(b), where the absolute value of cross section was achieved by analogy with Ref. [42]. The location of minimum $\gamma(\lambda)$ indeed blueshifts while Q_{solution} decreases. This explains the blueshift of multi-peak WGM emission shown in Fig. 6 qualitatively. However, we should emphasize here that Eq. (1) and Fig. 7 are only effective for multimode WGM emissions, as the leakage between fiber and cuvette is not included in the model.

On the contrary, the centers of the spectra do not shift for single-line emission (Fig. 6 left inset). This gives direct evidence that the single-mode emission, even if it originates from one of the whispering-gallery modes, does not share the same mechanism as multimode WGM emission. Other evidence for the ineffectiveness of Eq. (1) and Fig. 7 in explaining single-mode emission is that the shape of the $\gamma(\lambda)$ function is flatter at minimum for longer wavelengths (higher Q_{solution}), suggesting the appearance of more peaks while lasing. Although the precise mechanism behind single-mode emission and its relation with the theoretical models of an evanescent-wave-pumped WGM laser is still under investigation, we could suggest the following ideas by analyzing one of the crucial parameters describing the lasing process: the quality factor Q of the cavity. We noted experimentally that the single-mode emission could be observed when the fiber touches the cuvette wall and the RI of the solution is low. When the fiber is separated with the cuvette wall (the case for Fig. 5), or when the fiber touches the wall but the RI of the solution is high (the case for upper curves in Fig. 6), the multimode emission happens. Therefore, the single-mode or multimode emission relies on the competition of the following two loss mechanisms: one is the leak to cuvette through the coupling between fiber and cuvette, which may be described as Q_{cuvette}; the other (Q_{solution}) is the loss to the solution due to the evanescent wave. Q_{solution} is determined by the refractive index differences (Δn) between the solution and the fiber. Q_{cuvette}, the leakage to the cuvette, should be much less sensitive to the Δn. The Q could be simply expressed as $1/Q = 1/Q_{\text{solution}} + 1/Q_{\text{cuvette}}$, where Q_{cuvette} is assumed to be constant for the given configuration. Therefore, when the Δn is large, the $Q_{\text{solution}} > Q_{\text{cuvette}}$, and then Q could be mainly determined by Q_{cuvette}, so the laser mode does not change. We could take the attachment of cuvette and fiber as "perturbation" [43], which perturbs lasing modes to decrease the amplification of spontaneous emission. This would leave a much smaller number of lasing modes in the cavity compared to regular WGMs. Therefore, it is possible that only one lasing mode satisfies the lasing condition near the lowest threshold. Also, the lack of lasing modes will make more excitons available to contribute to lasing, resulting in a smaller lasing threshold [43]. On the contrary, when the Δn is small, $Q_{\text{solution}} < Q_{\text{cuvette}}$, the Q could be mainly determined by Q_{solution}, and then the laser mode is determined by the leakage to the solution as a pure cylindrical microcavity described in Ref. [27] and in Fig. 7, which also explains the blueshift of the multimode WGM emission explicitly. Unfortunately, due to the bad resolution of the system (~0.1 nm) in the current

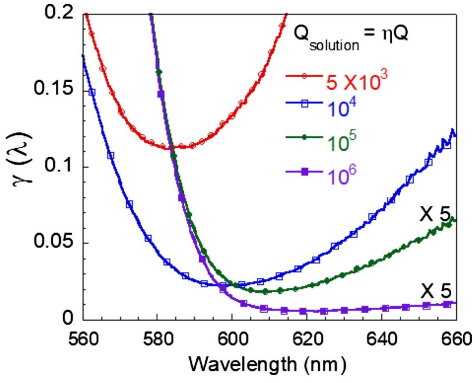

Fig. 7. Plot of $\gamma(\lambda)$, which is the fraction of the excited molecules at the laser threshold for various $Q_{\text{solution}} = \eta Q$; Q is the quality factor of the cavity, and η is the occupation factor, which is defined as the fraction of the evanescent field volume to that of the whole WGM [27].

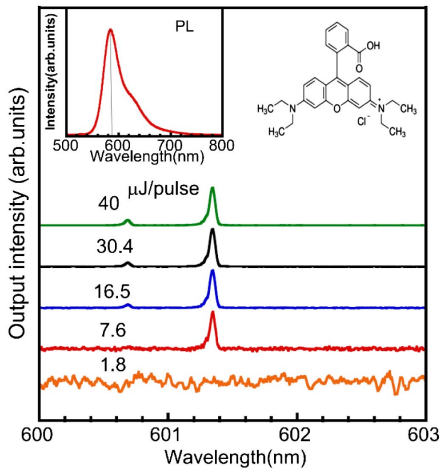

Fig. 8. Emission spectra from a fiber in 5 mg/mL rhodamine B ethanol solution at various excitation intensities with the same sample configuration as in Fig. 2(a). Left inset: PL spectrum of the solution excited at 20 mW/cm^2; right inset: molecular structure of rhodamine B.

work, we cannot observe the obvious change of Q values with different RIs of solutions. From the spectra in Fig. 6, the Q value can only be estimated as no less than ~6000, which, however, is much smaller than the theoretical and other experimental works using similar configurations [27].

To test the universality of our work, we also measured the WGM using 5 mg/mL rhodamine B ethanol solution as the gain solution, and a single-mode WGM was observed as that in rhodamine 6G ethanol solution. As shown in Fig. 8 left inset, its PL spectrum contains a main peak at 584 nm and a shoulder at 630 nm. At low pump energy, its spectrum is similar to the PL spectrum, and as the pump energy was increased to 7.6 μJ/pulse, a single-mode laser at 601.32 nm with FWHM of 0.1 nm was obtained. When the intensity increases, a second peak at 600.69 nm appears. But there is no multi-peak WGM emission observed. The results indicate the single-mode emission can not only be achieved in the rhodamine 6G ethanol solution but also exists in other solutions of gain medium with proper refractive index.

4. CONCLUSION

In conclusion, using a fiber with a 125 μm diameter and a dye solution with lower RI than that of the fiber, we have demonstrated controllable single- and multi-WGM optofluidic lasers based on evanescent-wave-coupled gain; the controllability was achieved by adjusting the distance between fiber and cuvette as well as the differences between the RIs of fiber and gain solution, i.e., the optical coupling between the cavity mode and its environments. Our work proves that controlling the leakage of the evanescent wave from high-Q microcavities will be crucial and will be useful for achieving desired optofluidic lasers, in particular, for single-mode emission.

Funding. National Natural Science Foundation of China (NSFC) (61574078, 61627802, 61704063); Fundamental Research Funds for the Central Universities (30915011202, 30916014112-002); Project of Jiangsu Laboratory of Lake Environment Remote Sensing Technologies (JSLERS-2017-001).

REFERENCES

1. F. Vollmer and S. Arnold, "Whispering-gallery-mode biosensing: label-free detection down to single molecules," Nat. Methods **5**, 591–596 (2008).
2. S. Avino, A. Krause, R. Zullo, A. Giorgini, P. Malara, P. De Natale, H. P. Loock, and G. Gagliardi, "Direct sensing in liquids using whispering-gallery-mode droplet resonators," Adv. Opt. Mater. **2**, 1155–1159 (2014).
3. Y. F. Xiao, S. H. Huang, S. Sheth, E. Jain, X. F. Jiang, S. P. Zustiak, and L. Yang, "Whispering gallery mode resonator sensor for *in situ* measurements of hydrogel gelation," Opt. Express **26**, 51–62 (2018).
4. Y. Y. Zhi, X. C. Yu, Q. H. Gong, L. Yang, and Y. F. Xiao, "Single nanoparticle detection using optical microcavities," Adv. Mater. **29**, 1604920 (2017).
5. D. K. Armani, T. J. Kippenberg, S. M. Spillane, and K. J. Vahala, "Ultra-high-Q toroid microcavity on a chip," Nature **421**, 925–928 (2003).
6. X. F. Jiang, L. B. Shao, S. X. Zhang, X. Yi, J. Wiersig, L. Wang, Q. H. Gong, M. Lončar, L. Yang, and Y. F. Xiao, "Chaos-assisted broadband momentum transformation in optical microresonators," Science **358**, 344–347 (2017).
7. S. Honghi and L. Feng, "Unidirectional lasing in semiconductor microring lasers at an exceptional point [Invited]," Photon. Res. **5**, B1–B6 (2017).
8. P. T. Snee, Y. Chan, D. G. Nocera, and M. G. Bawendi, "Whispering-gallery-mode lasing from a semiconductor nanocrystal/microsphere resonator composite," Adv. Mater. **17**, 1131–1136 (2005).
9. X. F. Jiang, C. L. Zou, L. Wang, Q. H. Gong, and Y. F. Xiao, "Whispering-gallery microcavities with unidirectional laser emission," Laser Photon. Rev. **10**, 40–61 (2016).
10. S. Yang, Y. Wang, and H. Sun, "Advances and prospects for whispering gallery mode microcavities," Adv. Opt. Mater. **3**, 1136–1162 (2015).
11. V. D. Ta, R. Chen, and H. D. Sun, "Tuning whispering gallery mode lasing from self-assembled polymer droplets," Sci. Rep. **3**, 1362 (2013).
12. S. Kushida, D. Okada, F. Sasaki, Z.-H. Lin, J. S. Huang, and Y. Yamamoto, "Low-threshold whispering gallery mode lasing from self-assembled microspheres of single-sort conjugated polymers," Adv. Opt. Mater. **5**, 1700123 (2017).
13. S. L. McCall, A. F. J. Levi, R. E. Slusher, S. J. Pearton, and R. A. Logan, "Whispering-gallery mode microdisk lasers," Appl. Phys. Lett. **60**, 289–291 (1992).
14. X. F. Jiang, Y. F. Xiao, C. L. Zou, L. He, C. H. Dong, B. B. Li, Y. Li, F. W. Sun, L. Yang, and Q. H. Gong, "Highly unidirectional emission and ultralow-threshold lasing from on-chip ultrahigh-Q microcavities," Adv. Mater. **24**, OP260–OP264 (2012).
15. Y. Kawabe, C. Spiegelberg, A. Schülzgen, M. F. Nabor, B. Kippelen, E. A. Mash, P. M. Allemand, M. Kuwata-Gonokami, K. Takeda, and N. Peyghambarian, "Whispering-gallery-mode microring laser using a conjugated polymer," Appl. Phys. Lett. **72**, 141–143 (1998).
16. C. Zhang, C. L. Zou, Y. L. Yan, C. Wei, J. M. Cui, F. W. Sun, J. N. Yao, and Y. S. Zhao, "Self-assembled organic crystalline microrings as active whispering-gallery-mode optical resonators," Adv. Opt. Mater. **1**, 357–361 (2013).
17. L. Shang, L. Y. Liu, and L. Xu, "Single-frequency coupled asymmetric microcavity laser," Opt. Lett. **33**, 1150–1152 (2008).
18. H. Li, L. Shang, X. Tu, L. Liu, and L. Xu, "Coupling variation induced ultrasensitive label-free biosensing by using single mode coupled microcavity laser," J. Am. Chem. Soc. **131**, 16612–16613 (2009).
19. T. Grossmann, T. Wienhold, U. Bog, T. Beck, C. Friedmann, H. Kalt, and T. Mappes, "Polymeric photonic molecule super-mode lasers on silicon," Light Sci. Appl. **2**, e82 (2013).
20. V. D. Ta, R. Chen, and H. D. Sun, "Coupled polymer microfiber lasers for single mode operation and enhanced refractive index sensing," Adv. Opt. Mater. **2**, 200–225 (2014).
21. L. Feng, Z. J. Wong, R. M. Ma, Y. Wang, and X. Zhang, "Single-mode laser by parity-time symmetry breaking," Science **346**, 972–975 (2014).
22. H. Hodaei, M. A. Miri, M. Heinrich, D. N. Christodoulides, and M. Khajavikhan, "Parity-time-symmetric microring lasers," Science **346**, 975–978 (2014).
23. F. Gu, F. Xie, X. Lin, S. L. Hu, and W. Fang, "Single whispering-gallery-mode lasing in polymer bottle microresonators via spatial pump engineering," Light Sci. Appl. **6**, e17061 (2017).
24. S. I. Shopova, H. Zhou, X. Fan, and P. Zhang, "Optofluidic ring resonator based dye laser," Appl. Phys. Lett. **90**, 221101 (2007).
25. S. Lacey, I. M. White, Y. Sun, S. I. Shopova, J. M. Cupps, P. Zhang, and X. Fan, "Versatile opto-fluidic ring resonator lasers with ultra-low threshold," Opt. Express **15**, 15523–15530 (2007).
26. L. He, S. K. Özdemir, and L. Yang, "Whispering gallery microcavity lasers," Laser Photon. Rev. **7**, 60–82 (2013).
27. H. J. Moon, Y. T. Chough, and K. An, "Cylindrical microcavity laser based on the evanescent-wave-coupled gain," Phys. Rev. Lett. **85**, 3161–3164 (2000).
28. M. Kazes, D. Y. Lewis, Y. Ebenstein, T. Mokari, and U. Banin, "Lasing from semiconductor quantum rods in a cylindrical micro-cavity," Adv. Mater. **14**, 317–321 (2002).
29. H. J. Moon, G. W. Park, S. B. Lee, K. An, and J. H. Lee, "Waveguide mode lasing via evanescent-wave-coupled gain from a thin cylindrical shell resonator," Appl. Phys. Lett. **84**, 4547–4549 (2004).
30. F. Lahoz, C. J. Oton, D. López, J. Marrero-Alonso, A. Boto, and M. Díaz, "Whispering gallery mode laser based on antitumor drug-dye complex gain medium," Opt. Lett. **37**, 4756–4758 (2012).

31. Y. Sun, S. I. Shopova, C. S. Wub, S. Arnold, and X. Fan, "Bioinspired optofluidic FRET lasers via DNA scaffolds," Proc. Natl. Acad. Sci. USA **107**, 16039–16042 (2010).
32. Y. Panitchob, G. Senthil Murugan, M. N. Zervas, P. Horak, S. Berneschi, S. Pelli, G. Nunzi Conti, and J. S. Wilkinson, "Whispering gallery mode spectra of channel waveguide coupled microspheres," Opt. Express **16**, 11066–11076 (2008).
33. H. Schmidt and A. R. Hawkins, "The photonic integration of non-solid media using optofluidics," Nat. Photonics **5**, 598–604 (2011).
34. F. Lahoz, "Thermally induced whispering gallery mode laser in MEH-PPV solutions," Organ. Electron. **15**, 1923–1927 (2014).
35. Y. X. Zhang, X. Y. Pu, L. Feng, D. Y. Han, and Y. T. Ren, "Polarization characteristics of whispering-gallery-mode fiber lasers based on evanescent-wave-coupled gain," Opt. Express **21**, 12617–12628 (2013).
36. K. Zhu, L. Feng, X. Y. Pu, and Y. X. Zhang, "Threshold property of whispering-gallery-mode fiber lasers pumped by evanescent waves," J. Opt. Soc. Am. B **28**, 2048–2056 (2011).
37. C. X. Sheng, R. C. Polson, Z. V. Vardeny, and D. A. Chinn, "Studies of π-conjugated polymer coupled microlasers," Synthetic Met. **135**, 147–149 (2003).
38. R. C. Polson, Z. V. Vardeny, and D. A. Chinn, "Multiple resonances in microdisk lasers of π-conjugated polymers," Appl. Phys. Lett. **81**, 1561–1563 (2002).
39. Y. Wang, X. Yang, H. Li, and C. Sheng, "Bright single-mode random laser from a concentrated solution of π-conjugated polymers," Opt. Lett. **41**, 269–272 (2016).
40. R. G. Hunsperger, *Theory of Optical Waveguides* (Springer, 2009).
41. D. L. Woerdeman and R. S. Parnas, "Model of a fiber-optic evanescent-wave fluorescence sensor," Appl. Spectrosc. **55**, 331–337 (2001).
42. P. Hammond, "Comparison of experimental and theoretical excited-state spectra for rhodamine 6G," IEEE J. Quantum Electron. **16**, 1157–1160 (1980).
43. S. A. Backe, J. R. A. Cleaver, A. P. Heberle, J. J. Baumberg, and K. Kohler, "Threshold reduction in pierced microdisk lasers," Appl. Phys. Lett. **74**, 176–178 (1999).